

Immunopathology and Infectious Diseases

Osteopontin Mediates *Citrobacter rodentium*-Induced Colonic Epithelial Cell Hyperplasia and Attaching-Effacing Lesions

Eytan Wine,* Grace Shen-Tu,^{†‡}
Mélanie G. Gareau,^{†‡} Harvey A. Goldberg,[§]
Christoph Licht,^{†‡} Bo-Yee Ngan,^{†‡}
Esben S. Sorensen,[¶] James Greenaway,[‡]
Jaro Sodek,[‡] Ron Zohar,[‡] and
Philip M. Sherman^{†‡}

From Pediatric Gastroenterology,* University of Alberta, Edmonton, Alberta, Canada; the Research Institute,[†] Hospital for Sick Children, University of Toronto,[‡] Toronto, Ontario, Canada; the Canadian Institutes of Health Research Group in Skeletal Development and Remodeling,[§] School of Dentistry, University of Western Ontario, London, Ontario, Canada; and the Department of Molecular Biology,[¶] University of Aarhus, Denmark

Although osteopontin (OPN) is up-regulated in inflammatory bowel diseases, its role in disease pathogenesis remains controversial. The objective of this study was to determine the role of OPN in host responses to a non-invasive bacterial pathogen, *Citrobacter rodentium*, which serves as a murine infectious model of colitis. OPN gene knockout and wild-type mice were infected orogastrically with either *C. rodentium* or Luria-Bertani (LB) broth. Mouse-derived OPN^{+/+} and OPN^{-/-} fibroblasts were incubated with *C. rodentium* and attaching-effacing lesions were demonstrated using transmission electron microscopy and immunofluorescence. Colonic expression of OPN was increased by *C. rodentium* infection of wild-type mice. Furthermore, colonic epithelial cell hyperplasia, the hallmark of *C. rodentium* infection, was reduced in OPN^{-/-} mice, and spleen enlargement by infection was absent in OPN^{-/-} mice. Rectal administration of OPN to OPN^{-/-} mice restored these effects. There was an 8- to 17-fold reduction in bacterial colonization in OPN^{-/-} mice, compared with wild-type mice, which was accompanied by reduced attaching-effacing lesions, both in infected OPN^{-/-} mice and OPN^{-/-} mouse fibroblasts. Moreover, adhesion pedestals were restored in OPN^{-/-} cells complemented with human OPN. Therefore, lack of OPN results in decreased pedestal formation, colonization, and colonic epithelial cell hyperplasia responses to *C. rodentium*

infection, indicating that OPN impacts disease pathogenesis through bacterial attachment and altered host immune responses. (Am J Pathol 2010, 177:1320–1332; DOI: 10.2353/ajpath.2010.091068)

Osteopontin (OPN) is a multifunctional glycoprotein involved in a variety of cellular functions, including stimulation of T helper(α)1 cytokines and adhesion through binding to integrins and CD44 receptors on cell surfaces. This cytokine is highly expressed in chronic inflammatory and autoimmune diseases¹ and is localized in and around inflammatory cells.² OPN is believed to exacerbate inflammation in a variety of settings, including infectious diseases.¹ It is involved in recruiting inflammatory cells to sites of injury, as indicated by a decrease in macrophage infiltration in ischemic kidneys in OPN-deficient (OPN^{-/-}) mice.¹ OPN is also involved in controlling expression of inflammatory mediators, such as down-regulation of the anti-inflammatory cytokine interleukin (IL)-10 and an increase in levels of the T_H1 cytokine interferon (IFN)γ.³

Accumulating evidence indicates that defects in the dynamic balance between organisms in the commensal intestinal microbiota and host innate defensive responses at the intestinal mucosal surface results in the induction of inflammatory bowel diseases (IBD).⁴ An association between luminal bacteria and IBD is further supported by

Supported by operating grants from the Canadian Institutes of Health Research (P.M.S., H.A.G., J.S., R.Z.), the Dairy Farmers of Canada (H.A.G., J.S., R.Z.) and the Danish Dairy Research Foundation (E.S.S.). E.W. was supported by a fellowship award from the Canadian Association of Gastroenterology/CIHR/Astra Zeneca partnership. G.S. is the recipient of a Canadian Institutes of Health Research Canada Graduate Scholarship Doctoral Research Award. P.M.S. is the recipient of a Canada Research Chair in Gastrointestinal Disease.

E.W. and G.S.-T. contributed equally to this work.

Accepted for publication May 20, 2010.

None of the authors disclosed any relevant financial relationships.

Address reprint requests to Philip M. Sherman, M.D., FRCPC, Hospital for Sick Children, Room 8409, 555 University Avenue, Toronto, Ontario, Canada, M5G 1X8. E-mail: philip.sherman@sickkids.ca.

animal models,⁵ including the use of *Citrobacter rodentium* infection. *C. rodentium* is the causative agent of transmissible murine colonic epithelial cell hyperplasia that harbors a locus of enterocyte effacement pathogenicity island, similar to enterohemorrhagic *Escherichia coli* (EHEC) O157:H7, and is capable of forming dense F-actin bacterial attachment pedestals, known as attaching-effacing (A/E) lesions, in mouse colon.⁶ The resulting T_H1 response and accompanying pathological changes represent findings observed in patients with IBD.⁷ As a result, *C. rodentium* serves as a relevant animal model to study potential infectious mechanisms of IBD.⁸

An association between OPN and IBD was recently assessed using dextran sodium sulfate (DSS) to induce colitis in wild-type and OPN^{-/-} mice. However, the results arising were contradictory. One study suggested that lack of OPN has a protective effect,⁹ whereas others reported a detrimental outcome during the acute phase¹⁰⁻¹² and protection from chronic exposure to DSS.¹¹ This controversy prompted us to study an association between OPN and gut inflammation, using *C. rodentium* as a model of infectious colitis, to provide insight regarding the role of OPN in the pathogenesis of IBD.

Herein, we describe the attenuation of *C. rodentium*-induced colonic epithelial cell hyperplasia and a reduction in bacterial colonization in OPN^{-/-} mice. In addition, we demonstrate dependence of adhesion pedestal formation in response to *C. rodentium* on the presence of OPN. Taken together, these findings contribute to an improved understanding of the role of OPN in response to intestinal infection.

Materials and Methods

Mice

OPN^{-/-} mice, kindly provided by Dr. Susan Rittling (Forsyth Institute, MA) and Dr. David Denhardt (Rutgers University, NJ), back-crossed into a C57BL/6 background, were generated and maintained, as described previously.¹³ All OPN^{-/-} mice and C57BL/6 control mice (6 to 8 weeks old) were maintained in a specific pathogen-free environment. The mice were transferred to a containment facility at least 3 days before pathogenic inoculation. Animal care and interventions were ap-

proved by the Hospital for Sick Children Laboratory Animal Services.

Bacterial Infection of Mice

C. rodentium, strain DBS100 (ATCC 51459, generously provided by the late Dr. David Schauer, Massachusetts Institute of Technology, Cambridge, MA) was stored in Luria-Bertani (LB) broth with 10% glycerol at -80°C. Bacteria were grown from frozen stocks on LB agar plates at 37°C and then re-grown in LB broth overnight at 37°C. The inoculum was prepared to reach a final infection suspension containing 10⁹ colony-forming units (CFU)/ml. Mice were inoculated by orogastric gavage with 0.1 ml of the bacterial suspension. Sham controls were challenged with an equal volume of sterile LB broth. In most cases, mice were maintained until postinfection (PI) day 10. In some experiments animals were euthanized on PI days 3, 6, and 15 for tissue analyses and to establish the time-course of OPN responses and bacterial colonization to infection.

In a subset of experiments, OPN purified from bovine milk, was either added to the drinking water, to reach a concentration of 20 µg/ml,¹⁴ or inserted into the rectum of wild-type and OPN^{-/-} mice without anesthesia once a day (2 µg in 100 µl PBS) through a flexible plastic cannula. In all cases, OPN supplementation was started 24 hours before infection and maintained throughout the 10 days of infection, until sacrifice. PBS was rectally inserted to control mice (to control for potential confounding effects of daily rectal insertion).

Large Bowel Histology and Immunohistochemistry

Large bowel sections were fixed in 10% buffered formalin and stained with hematoxylin and eosin (H&E). Intestinal inflammation was graded on coded sections by a single pathologist (B-YN; Table 1).¹⁵ Mucosal thickness and epithelial cell hyperplasia were assessed using a Zeiss Axioplan microscope and digital photographs (SenSys; Photometrics, Tucson, AZ). The average depth of 20 well-oriented colonic crypts was measured for each mouse (V for Windows; Digital Optics, Auckland, New Zealand).

Table 1. Colonic Inflammation Histological Score*

Criterion	Score				
	0	1	2	3	4
Goblet cells	—	↓	↓↓	↓↓↓	↓↓↓
Mucosal thickening	—	↑	↑↑	↑↑↑	↑↑↑
Inflammatory cells	—	↑	↑↑	↑↑↑	↑↑↑
Submucosa cell infiltration	—	—	↑	↑↑	↑↑↑
Destruction of architecture	—	—	—	↑	↑↑
Ulcers (epithelial cell surface)	0%	0–25%	25%–50%	50%–75%	75%–100%
Crypt abscesses	0	1–3	4–6	7–9	>10
Eosinophil infiltration	—	↑	↑↑	↑↑↑	↑↑↑

*Scoring criteria modified from Van der Sluis, et al.¹⁵

↑, increase in parameter; ↓, decrease in parameter. The number of arrows reflects the magnitude of change.

For immunohistochemistry, formalin-fixed, paraffin-embedded tissues were mounted onto positive-charged microscope slides and baked overnight at 60°C. Polyclonal rabbit anti-mouse cleaved caspase 3 antibody (Ab) (Cell Signaling Technology, Danvers, MA) and rabbit-monoclonal Ab against Ki-67 (Lab Vision, Fremont, CA) were used on an automated immune stainer (Benchmark, Ventana Medical Systems, Tucson, AZ) at dilutions of 1:40 and 1:100, respectively. Immunodetection was performed using a LSAB system using a 1:100 dilution of biotinylated anti-rabbit immunoglobulin (Ig)G (Vector Laboratories, Burlingame, CA) with a commercial secondary detection system (Ventana iVIEW DAB). Tissue sections were dewaxed, heat-induced epitope retrieved, peroxidase blocked, endogenous biotin blocked, and counterstained with hematoxylin.

For OPN immunohistochemistry, colonic sections were deparaffinized and heat-induced epitope retrieval was performed with Tris-EDTA, pH 9. Rabbit polyclonal anti-OPN Ab (reacts with human and mouse OPN; dilution 1:750; Abcam Inc., Cambridge, MA) was incubated for 1 hour, followed by incubation with secondary Ab and treatment with horseradish peroxidase-conjugated streptavidin as the labeling reagent. Color was developed with NovaRed solution and counterstained with hematoxylin.

Enzyme-Linked Immunosorbent Assay

Immediately after euthanasia, blood samples were obtained by cardiac puncture. Serum was collected on centrifugation at 18,000 × *g* for 10 minutes. Distal colonic sections were collected in 1 ml Complete protease inhibitor cocktail (Roche Diagnostics, Mannheim, Germany) and then homogenized. Samples were stored at -80°C until use. Osteopontin levels in serum samples and colonic homogenates were assessed using a mouse osteopontin immunoassay kit as per the manufacturer's instructions (R&D Systems Inc., Minneapolis, MN).

Immunoblotting

Aliquots of colonic homogenates were analyzed for OPN and β -actin. Proteins were separated by precasted 10% Tris-HCl (Bio-Rad, Hercules, CA) SDS polyacrylamide gel electrophoresis with a protein ladder standard (Bio-Rad, broad molecular range ladder). After electrophoresis, proteins were transferred onto nitrocellulose membranes (Pall Corporation, Pensacola, FL) and incubated in Odyssey® blocking buffer (LI-COR Biosciences, Lincoln, NE) before probing with polyclonal rabbit anti-human OPN Ab (also reacts with mouse OPN; Abcam; 1:1000) and primary mouse monoclonal IgG Ab against β -actin (Sigma, Saint Louis, Missouri; 1:5000) overnight. After washing the membrane (PBS plus 0.1% Tween-20), blots were incubated with Ab [IRDye 800 goat anti-rabbit IgG (Rockland Immunochemicals, Gilbertsville, PA; 1:20,000) and Alexa Fluor 680 goat anti-mouse IgG (Invitrogen, Carlsbad, CA)] and incubated for 1 hour at room temperature on a shaker. The blots were then washed and the membrane was scanned; bands were detected using the Odyssey system (LI-COR Bio-

sciences). The integrative intensities of the detected bands were obtained by software (Odyssey Infrared Imaging System, LI-COR Biosciences). Quantification of osteopontin expression was obtained by normalizing the integrated intensity of the OPN band with β -actin expression.

mRNA Expression of OPN Using Quantitative Real-Time PCR

Quantitative real-time PCR was used to quantify expression of OPN in colons of wild-type animals infected with *C. rodentium* and sham controls. Briefly, colonic tissues were snap-frozen in liquid nitrogen and stored at -80°C until further use. Total RNA was isolated by homogenization in TRIzol reagent (Invitrogen), phase separation using chloroform extraction, and precipitation from the aqueous phase using isopropyl alcohol. Washed RNA was re-dissolved in RNase-free water and stored at -80°C. RNA was treated with DNase1 (Invitrogen) according to the manufacturer's instructions. cDNA was synthesized using the iScript synthesis kit (Bio-Rad) and stored at -20°C. PCR was performed using SYBR green reagents (Bio-Rad) and validated primers for β -actin (Forward: 5'-GGCTGTATTCCCCTCCATCG-3'; Reverse: 5'-CCAGTTGGTAACAATGCCATGT-3') and for OPN (Forward: 5'-AGCAAGAAACTCTTCCAAGCAA-3'; Reverse: 5'-GTGAGATTCGTCAGATTCATCCG-3'; Invitrogen). Expression levels were normalized using β -actin as the reference gene and expressed as $\Delta\Delta CT$ values.

Cytokine Assay

Distal colons homogenates were used for mouse T_H1/T_H2/IL-17 cytokine detection using MESO Scale Discovery cytokine assay kits (Gaithersburg, Maryland). Samples were prepared according to manufacturer's protocol and levels of IFN γ , IL-1 β , IL-2, IL-4, IL-5, IL-10, IL-12, IL-17, Keratinocyte chemoattractant (KC), and tumor necrosis factor- α were quantified using electrochemiluminescence detection.

Weight, Stool Changes, and Bacterial Colonization

All mice were checked daily for the development of signs of morbidity. A disease activity index score (Table 2, scoring criteria modified from¹⁵) was obtained by documenting body weight, stool color and consistency and

Table 2. Modified Disease Activity Index Score*

Score	Weight loss %	Stool consistency	Blood loss	Appearance
0	None	Normal	Negative	Normal
1	1-5%	Loose		Hunched
2	5-10%	Diarrhea	Gross	Starey coat
3	10-15%			Lethargic
4	>15%			

*Scoring criteria modified from Van der Sluis, et al.¹⁵

general appearance every 3 days until euthanization by cervical dislocation on PI day 10. Rectal swabs were collected on the same days and plated onto MacConkey agar plates, and incubated aerobically overnight at 37°C. *C. rodentium* colonies were distinguished by their typical size and morphology.¹⁶ *C. rodentium* colonization was quantified on day 10 by homogenization of either fecal pellets or distal colonic tissue in 1 ml PBS and plating of 10-fold serial dilutions onto MacConkey agar. *C. rodentium* colonies were enumerated after overnight growth at 37°C, and results expressed as CFU/g feces or colonic tissue.

Detection of Bacterial Translocation

Blood samples were obtained by cardiac puncture, and the spleen, liver, and mesentery (including lymph nodes) removed, weighed, and homogenized (Pro200 homogenizer, PRO Scientific Inc., Oxford, CT). Under sterile conditions, aliquots (10 μ l) of blood or organ homogenate were plated in 10-fold serial dilutions onto blood agar plates and incubated aerobically for 24 hours at 37°C, after which the number of bacterial CFU was calculated per ml of blood or per gram of tissue.

Cells and Bacterial Infection

Wild-type, OPN^{-/-}, and OPN^{-/-} mouse fibroblasts complemented with human OPN¹⁷ were used as *in vitro* model systems and cultured in Dulbecco's Modified Eagle Medium (DMEM) with 10% fetal bovine serum, 100 μ g/ml penicillin G, 50 μ g/ml gentamicin, and 0.3 μ g/ml fungizone (37°C; 5% CO₂). OPN-rescued cells were supplemented with Geneticin (all reagents from Gibco Laboratories, Grand Island, NY). Cells, incubated in antibiotic-free medium overnight were infected with either EHEC O157:H7, strain CL56, (Hospital for Sick Children, Toronto, ON, Canada) or *C. rodentium* (multiplicity of infection 100:1; 37°C; 5% CO₂). In some experiments bovine milk OPN (5 μ g/ml)¹⁸ or recombinant OPN¹⁹ were added to the medium 1 hour before bacterial infection.

Transmission Electron Microscopy

Mouse fibroblasts were grown on six-well plates and infected with *C. rodentium* (multiplicity of infection 100:1) for 4 hours at 37°C. Cells or colonic tissue samples were then washed and fixed in 4% paraformaldehyde + 1% glutaraldehyde in PBS, postfixed in 1% osmium tetroxide, dehydrated in a graded series of acetone, and subsequently infiltrated and embedded in Epon-Araldite epoxy resin. The processing steps from post fixation to polymerization of resin blocks were performed in a microwave oven (Pelco BioWave 34770, Pelco International, Redding, CA), as recommended by the manufacturer. Ultra-thin sections were cut with a diamond knife (Reichert Ultracut E, Leica Inc, Wetzlar, Germany). Sections were stained with uranyl acetate and lead citrate before being examined by transmission electron microscopy (JEM-1011, JEOL USA Corp., Peabody, MA). Digital electron

micrographs were acquired directly with a 1024 \times 1024 pixels CCD camera system (AMT Corp., Denver, MA).

Immunofluorescence

Mouse fibroblasts were grown on glass 22 \times 22 mm No.1.5 coverslips (VWR LabShop, Vatabia, IL) in 6-well plates covered with 2 ml of antibiotic-free media. Cells were infected with EHEC or *C. rodentium* at multiplicity of infection of 100:1 for 4.5 to 6 hours. Slides were washed, fixed (paraformaldehyde), permeabilized (Triton-X 100), blocked for 30 minutes with 0.1% bovine serum albumin, and incubated in fluorescein isothiocyanate-conjugated polyclonal goat-anti-EHEC O175:H7 Ab (1:100; Fitzgerald, Concord, MA) or rabbit-anti-*C. rodentium* Ab with Alexa Fluor 594 Phalloidin for 1 hour. Goat anti-rabbit Cy2 secondary Ab (1:100; 1 hour; 20°C; Jackson Immunoresearch Inc., West Grove, PA) was used to visualize *C. rodentium*. Slides were stained with DAPI for 5 minutes before 3 washes with PBS and then mounted using SlowFade Antifade Kits (Molecular Probes, Eugene, OR) and analyzed under alternating phase-contrast and fluorescence microscopy (Leitz Dialux 22; Leica Canada, Inc., Toronto, ON, Canada).

Adhesion Assay

Mouse fibroblasts were grown in antibiotic-free culture medium in 6-well plates overnight. Cells were then infected with 10⁸ bacteria (multiplicity of infection 100:1) for 4.5 hours in 5% CO₂ at 37°C. After infection, nonadherent bacteria were removed by washing the monolayers three times with PBS (pH 7.0). Triton X-100 (0.1%, diluted in PBS) was added to each well and left on an orbital spinner for 15 minutes at room temperature. To quantify the number of bacteria adherent to cells, serial dilutions were performed on each sample by taking 10 μ l from a series of 10-fold diluted samples plating onto blood agar plates and cultured overnight in 37°C. The number of bacteria on each plate was then counted to calculate the original number of adherent bacteria.

Statistics

Results are expressed as means \pm SEM. Analysis of variance and unpaired Student's *t*-test were used, as appropriate, with Tukey's posthoc test for normal distribution was ascertained, and nonparametric Kruskal-Wallis test for non-normal distribution. Fisher's exact test was used for analysis of categorical data. Analyses were conducted using InStat3 (GraphPad, San Diego, CA). *P* < 0.05 was considered significant.

Results

C. rodentium Infection Increases OPN Expression in Mouse Colons

Wild-type C57BL/6 and OPN^{-/-} mice (*N* = 31 & 28, respectively) were challenged orogastrically with *C. ro-*

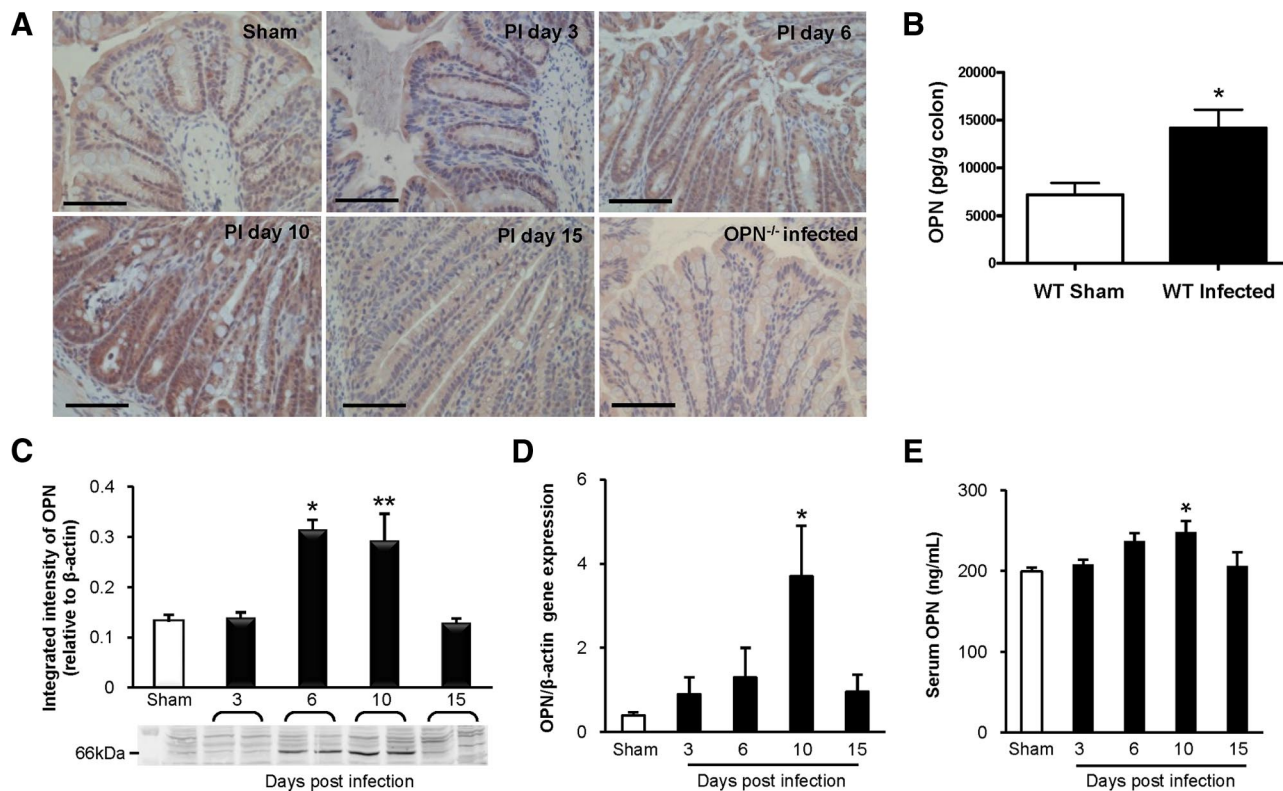


Figure 1. OPN expression is increased in response to *C. rodentium* infection. **A:** Colonic immunohistochemistry showed that OPN was present at low levels in uninfected wild-type (WT) mice (**top left panel**), mainly located in the cytoplasm of surface epithelial cells. A time-dependent increase in OPN expression was observed throughout the crypts of *C. rodentium*-infected wild-type mice as the infection progressed to 10 days, followed by a reduction in OPN by PI day 15. Scale bar: 100 μ m. **B:** Enzyme-linked immunosorbent assay of wild-type mouse colons demonstrated a threefold increase in OPN levels with infection ($N = 4$ to 8; t -test: $*P < 0.005$). **C:** Western blotting of colonic homogenates of wild-type mice showed a similar increase in OPN protein level, normalized to β -actin, on PI day 6 ($N = 4$ to 5; analysis of variance: $*P < 0.01$) and on PI day 10 (t -test: $**P < 0.05$). **D:** Colonic mRNA levels of OPN, relative to β -actin, showed increased OPN expression in infected colons on PI day 10 by qPCR ($N = 5$ to 9; analysis of variance: $*P < 0.01$). **E:** Serum OPN levels, as measured by enzyme-linked immunosorbent assay, were increased on PI day 10 and normalized by PI day 15 ($N = 5$ to 9; analysis of variance: $*P < 0.05$).

dentium (10^8 CFU/0.1 ml), and 16 to 20 additional mice in each group were used as sham-infected controls. Experiments were conducted on at least four separate occasions. To determine whether OPN mediates epithelial responses to *C. rodentium*, the effect of bacterial infection on OPN expression in the colon was assessed during the 10 day course of infection by immunohistochemistry, protein enzyme-linked immunosorbent assay and western blotting, and quantitative PCR. As expected, colons from OPN^{-/-} mice did not stain positive for OPN, whereas uninfected wild-type mice (sham) had low basal levels of OPN, located mainly at the luminal surface (Figure 1A). Infection with *C. rodentium* led to a time-dependent increase in OPN expression throughout the entire length of the crypts that peaked at PI day 10, when inflammation is most prominent, and then decreased at PI day 15 (Figure 1A). OPN protein levels in colons increased by ~threefold during infection (Figure 1, B and C) and a 10-fold increase in OPN mRNA expression in colonic homogenates of infected wild-type mice after 10 days of infection (Figure 1D), as well as parallel increases in OPN serum (Figure 1E) were also observed. These findings support the involvement of OPN in epithelial cell responses to infection, as shown in inflamed colons of human subjects with IBD.^{20,21}

OPN Is Associated with Inflammation and Colonic Epithelial Cell Hyperplasia in Response to *C. rodentium* Infection

Colonic epithelial cell hyperplasia, the hallmark of the host response to *C. rodentium* infection,²² was demonstrated by a doubling in crypt length in 10 day-infected wild-type mice (290 ± 6 vs. $144 \pm 4 \mu$ m in wild-type sham; Figure 2A and B; $P < 0.001$). However, *C. rodentium* infection increased crypt length in OPN^{-/-} mice by only 21% (205 ± 8 vs. $169 \pm 4 \mu$ m in sham-OPN^{-/-} mice; $P < 0.05$), which was considerably shorter than in infected wild-type mice (Figure 2A and B; $P < 0.001$). Similarly, there were significant differences in histology scores, used as a reproducible measure of mucosal injury, between wild-type and OPN^{-/-} infected mouse colons (7.1 ± 1.1 vs. 3.9 ± 0.8 , respectively; Figure 2, C and D; $P < 0.05$). Cytokine levels, measured in mouse colon homogenates, showed increases in IFN γ , IL-1 β , and tumor necrosis factor- α levels with infection of wild-type mice ($P < 0.05$) but no increase in infected knockout mice ($P > 0.05$). IFN γ was higher in infected wild-type mice than in infected OPN^{-/-} mice (Figure 2 E; $P < 0.05$). There were no changes in levels of IL-2, IL-4, IL-5, IL-10, IL-17, or KC in both groups (data not shown).

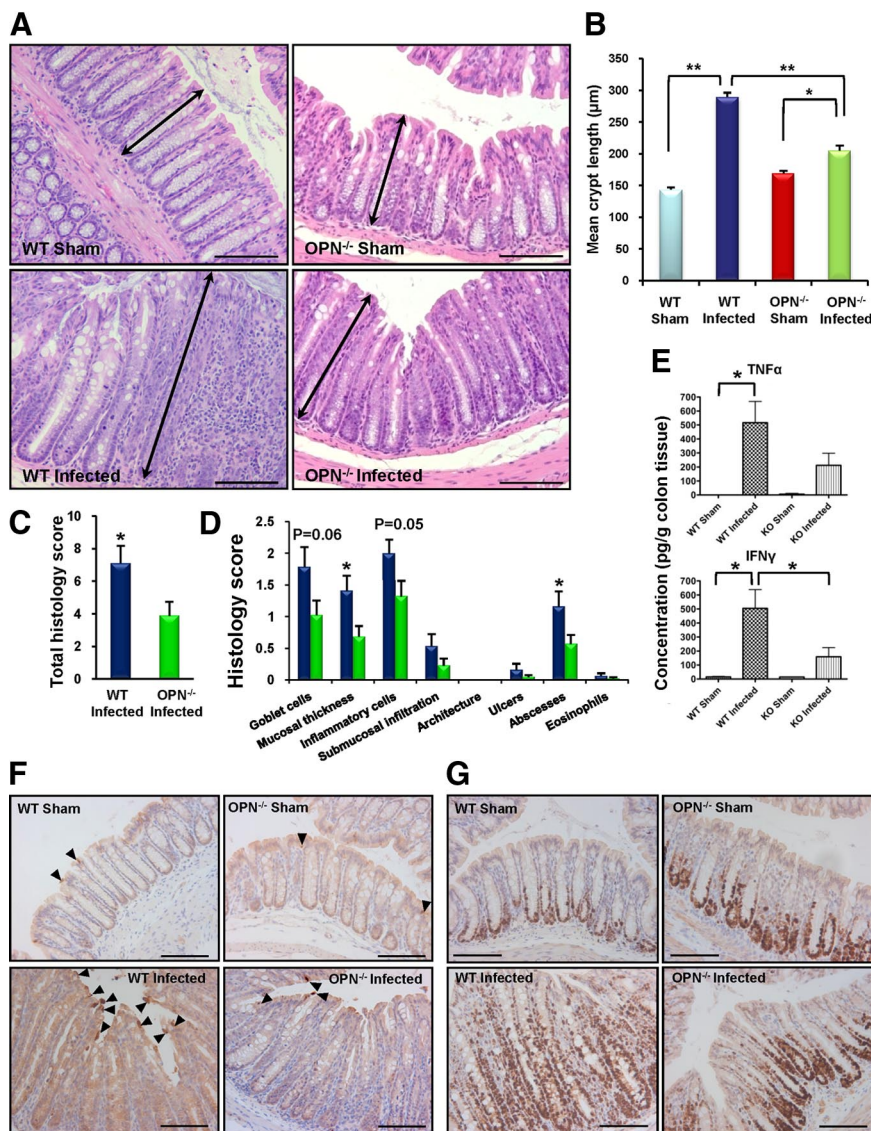


Figure 2. Colonic epithelial cell hyperplasia and inflammation in response to *C. rodentium* are associated with OPN. **A:** A decrease in the hyperplastic response after ten days of *C. rodentium* infection was observed in OPN^{-/-} infected mice (**bottom right panel**), relative to infected wild-type (WT) mice (**bottom left panel**). **Arrows** indicate crypt length. Scale bar: 100 µm. **B:** Quantification was performed by measuring colonic crypt length in 20 well-oriented crypts per mouse (*N* = 15 to 24; analysis of variance: **P* < 0.05; ***P* < 0.001). **C:** Overall histological grading of colitis (PI day 10) indicated higher scores in wild-type-infected relative to OPN^{-/-}-infected colons (*t*-test: **P* < 0.05). **D:** Breakdown of the histology score revealed increased severity in wild-type-infected mice (blue bars) relative to OPN^{-/-}-infected mice (green bars) with respect to mucosal thickening and abscess formation (*t*-test: **P* < 0.05) but no significant change in goblet cell displacement and inflammatory cell infiltration, which was mainly neutrophilic in nature (*P* = 0.06 and 0.05, respectively). **E:** Tumor necrosis factor-α and IFNγ were increased in colonic homogenates of infected wild-type mice (*t*-test: **P* < 0.05) but not OPN^{-/-} mice. IFNγ levels were higher in infected wild-type mice than in OPN^{-/-} mice (*t*-test: **P* < 0.05). **F:** Cleaved caspase-3 staining demonstrated a small number of apoptotic epithelial cells in uninfected wild-type and OPN^{-/-} mice (**arrowheads in top left and right panels**, respectively). Infection with *C. rodentium* resulted in an increase in apoptosis in wild-type mice (**arrowheads in bottom left panel**), but not in OPN^{-/-} mice (**bottom right panel**). **G:** In both uninfected wild-type and OPN^{-/-} mice (**top panels**) Ki-67 staining indicated that the proliferative zone was limited to the **bottom** third of colonic crypts. Infection with *C. rodentium* caused an increase in proliferation, which extended to the whole length of the crypt in wild-type colons (**bottom left panel**), but not in OPN^{-/-} mice (**bottom right panel**). Scale bar: 100 µm.

The reduced crypt epithelial cell hyperplasia in OPN^{-/-} mice in response to *C. rodentium* infection was due to a reduction in cell proliferative responses and not an increase in apoptosis (Figure 2, F and G).

C. rodentium Colonization of Mice Is Reduced in the Absence of OPN

OPN^{-/-} mice had significantly less *C. rodentium* CFU/g feces than infected wild-type mice ($1.2 \times 10^6 \pm 3.4 \times 10^5$ vs. $2.1 \times 10^7 \pm 5.6 \times 10^6$, respectively; Figure 3A; *P* < 0.005) after 10 days of infection, suggesting that OPN contributes to maintenance of *C. rodentium* colonization in the colon. There was also a reduction in bacteria in colonic tissue homogenates of infected OPN^{-/-} mice ($5.4 \times 10^5 \pm 1.4 \times 10^5$), relative to infected wild-type mice ($4.3 \times 10^6 \pm 1 \times 10^6$ CFU/g colon; Figure 3B; *P* < 0.005). A reduction in colonization of OPN^{-/-} mice, relative to wild-type mice, was

also observed on PI day 6 and bacterial clearance was apparent on PI day 15; findings that indicate that reduced pathogen colonization was not due to changes in the time-course of infection in OPN^{-/-} mice (Figure 3, C and D; *P* < 0.01). These results suggest that OPN^{-/-} mice were partially protected from *C. rodentium* infection due to a reduction in bacterial colonization in the absence of OPN. Consistent with previous reports,²² bacterial colonization of wild-type mice peaked at PI day 6 (Figure 3C).

Weight Loss and Disease Activity in Response to *C. rodentium* Infection Are Not Affected by OPN

Disease activity index (Table 2) scores for wild-type- and OPN^{-/-}-infected mice on days 4 and 10 were

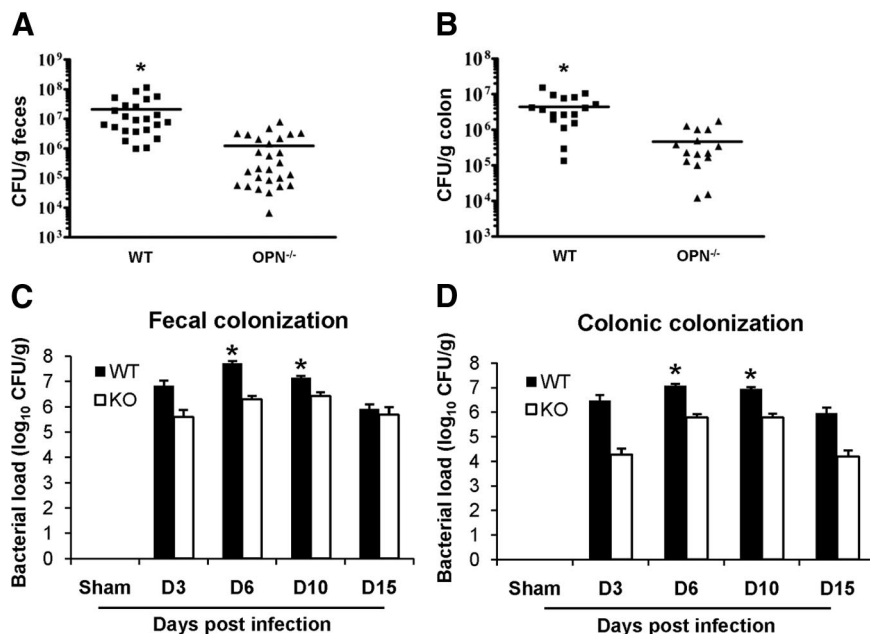


Figure 3. OPN mediates *C. rodentium* colonization. **A** and **B:** Colonization with *C. rodentium* on PI day 10 was measured by homogenizing fecal pellets and colonic tissues and then quantifying bacterial growth in serial dilutions. OPN^{-/-} mice infected with *C. rodentium* had significantly fewer CFU/g feces (**A**) and colonic homogenates (**B**), compared with infected wild-type (WT) mice (*t*-test: **P* < 0.005). **C** and **D:** A time-course of infection, quantifying CFU in feces (**C**) and colonic homogenates (**D**) of infected OPN^{-/-} mice relative to infected wild-type mice showed a similar pattern of peak colonization on days six and ten and a reduction in bacterial load on day 15 (**P* < 0.01). In wild-type mice, fecal colonization was maximum at six days PI (analysis of variance: *P* < 0.001 PI day six relative to all other time points; KO mice: *P* > 0.05).

higher than in sham mice (*P* < 0.05; data not shown). Ten days after challenge, both sham groups gained approximately 10% body weight, while weights of *C. rodentium*-infected wild-type and OPN^{-/-} mice remained unchanged. However, there was no difference in disease activity index between wild-type and OPN^{-/-} mice infected with *C. rodentium*. The lack of profound effect for OPN on systemic responses to infection is likely due to relatively mild systemic disease in C57BL/6 mice infected with *C. rodentium*, compared with other mouse strains.^{23,24}

Rectal OPN Supplementation Partially Restores Colonic Epithelial Cell Hyperplasia in Response to *C. rodentium* Infection in OPN^{-/-} Mice

To support our hypothesis that OPN is involved in colonic epithelial cell hyperplasia, bovine milk OPN was administered daily by rectal insertion to OPN^{-/-} mice. OPN alone had no effect on crypt length in sham-infected OPN^{-/-} mice (183 ± 3 vs. 168 ± 7 μm with rectal PBS). By contrast, rectal OPN given daily to OPN^{-/-} mice 24 hours before, and throughout the 10 day *C. rodentium* infection increased the colonic crypt length (256 ± 12 vs. 196 ± 20 μm in infected OPN^{-/-} mice that received PBS alone rectally; Figure 4A; *P* = 0.01). Although rectal delivery of exogenous OPN did not completely restore crypt length to levels observed in infected wild-type mice (Figure 2B), these results confirm a role for OPN in mediating epithelial cell responses to *C. rodentium* infection. In contrast, oral administration of OPN to infected OPN^{-/-} mice¹² did not increase crypt length (data not shown), possibly due to intraluminal degradation of exogenous protein.

Bacterial Translocation in Infected Mice Is Dependent on OPN

At PI day 10, there was a non-significant reduction in bacterial translocation to mesenteric lymph nodes of infected OPN^{-/-} mice (18%), relative to wild-type-infected mice (44%; Fisher's exact test: *P* = 0.09), while 50% of OPN-treated OPN^{-/-} mice had viable bacterial translocation to lymph nodes (Figure 4B). Bacterial translocation to the liver was higher in wild-type-infected mice and OPN-treated OPN^{-/-} mice than in OPN^{-/-} mice (*P* < 0.0001 and *P* < 0.01, respectively). Positive spleen cultures were uncommon and bacteremia was found in 50% of OPN-treated mice, but only two mice in each of the other infected groups (Figure 4B; *P* = 0.05). It is possible that the reduced bacterial translocation observed is a consequence of lower colonization seen in OPN^{-/-} mice. However, even though rectal OPN restored crypt hyperplasia responses to *C. rodentium* infection, pathogen colonization was not increased in OPN-treated versus PBS-treated mice (Figure 4, C and D; *P* > 0.05).

Increases in Spleen Weight and Splenocyte Numbers in Response to *C. rodentium* Infection Are Mediated by OPN

There was a 46% increase in the weight of spleens of infected wild-type mice on PI day 10 (133 ± 11 vs. 91 ± 7 mg in uninfected-wild-type; *P* < 0.005), likely due to accumulation of immune cells within the spleen after infection.²⁵ This effect was absent in OPN^{-/-} mice (93 ± 7 vs. 82 ± 6 mg in infected and uninfected mice, respectively; Figure 4E; *N* = 11 to 28). Daily rectal delivery of OPN to infected OPN^{-/-} mice restored

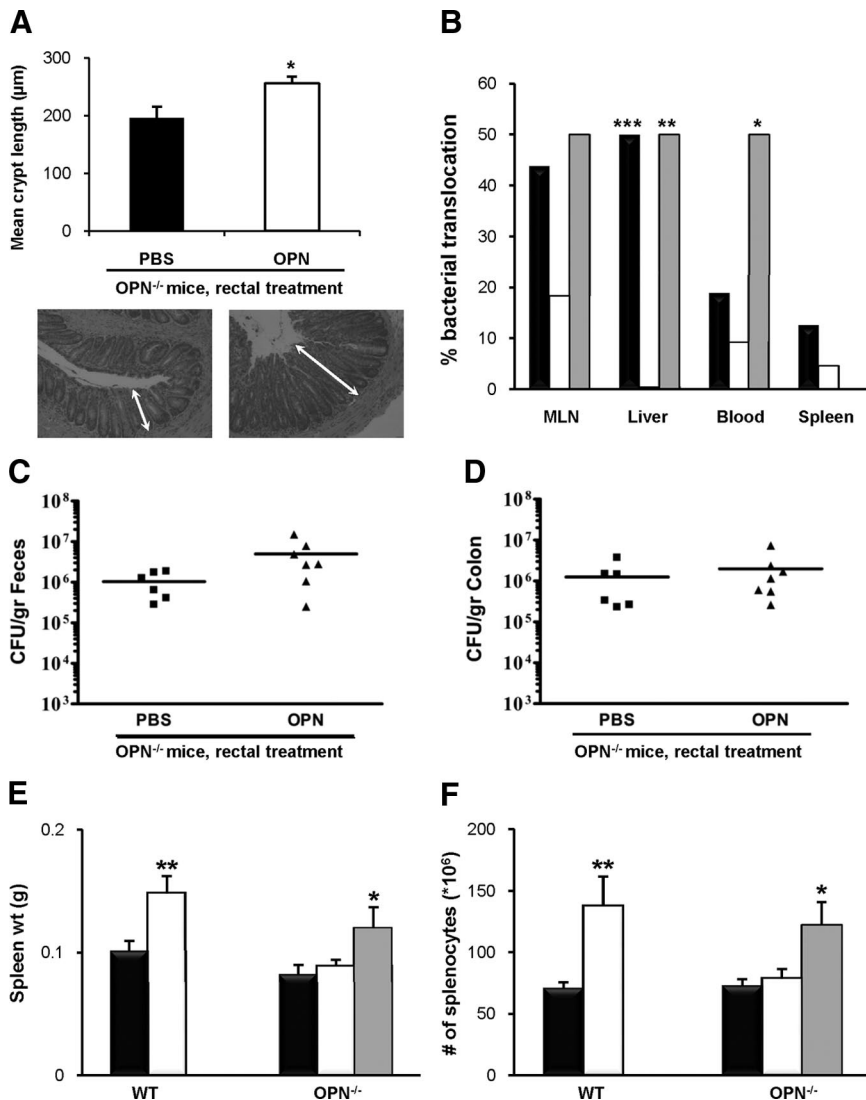


Figure 4. Rectal OPN restores responses to *C. rodentium* infection in $OPN^{-/-}$ mice. **A:** Quantification of colonic crypt length of $OPN^{-/-}$ mice receiving bovine milk OPN by daily rectal administration indicated a partial recovery in the phenotype with longer colonic crypts ($N = 8$ to 15 ; analysis of variance; $*P = 0.01$; representative micrographs below chart). **B:** Eighteen percent of infected $OPN^{-/-}$ mice (white bars) had bacterial translocation to the MLN, relative to 44% of infected wild-type (WT) mice (black bars; $P = 0.09$); translocation was restored in $OPN^{-/-}$ mice pretreated with rectal OPN (gray bars). Bacterial translocation to the liver was higher in wild-type and rectal OPN-treated mice than in infected $OPN^{-/-}$ mice (Fisher's exact test: $**P < 0.01$ $***P < 0.0001$), and bacteremia was more common in mice treated with rectal OPN ($*P < 0.05$). **C and D:** Fecal (**C**) and colonic (**D**) evidence of *C. rodentium* colonization was not increased in $OPN^{-/-}$ mice pretreated with rectal OPN ($P = 0.09$ and 0.5 , respectively). **E:** An increase was observed in the weight of spleens from *C. rodentium*-infected wild-type mice (white bars in panels **E** and **F**), relative to uninfected wild-type mice (black bars; $N = 12$ and 8 ; analysis of variance: $**P < 0.001$). While infection of $OPN^{-/-}$ mice did not change the size of the spleen, topical rectal OPN given to $OPN^{-/-}$ mice infected with *C. rodentium* led to an increase in spleen weights (gray bars; $N = 6$; $*P < 0.05$). **F:** The number of splenocytes in wild-type mice doubled following *C. rodentium* infection (analysis of variance: $**P < 0.01$). There was no change in the splenocyte counts in $OPN^{-/-}$ mice in response to enteric infection, but the addition of daily rectal OPN to $OPN^{-/-}$ mice produced a response similar to levels seen in infected wild-type mice ($*P < 0.05$).

spleen weights to levels similar to infected wild-type mice (120 ± 17 mg).

There was a parallel increase in the number of splenocytes in wild-type mice from $88 \pm 15 \times 10^6$ to $159 \pm 19 \times 10^6$ cells/spleen following *C. rodentium* infection ($P < 0.01$). Such an increase was absent in $OPN^{-/-}$ mice ($78 \pm 5 \times 10^6$ vs. $85 \pm 7 \times 10^6$ with infection; Figure 4F), whereas rectal treatment of OPN to $OPN^{-/-}$ mice increased the number of splenocytes to $122 \pm 19 \times 10^6$ ($P < 0.05$). There was no difference between uninfected wild-type and $OPN^{-/-}$ mice in spleen weights or numbers of splenocytes. These findings suggest that OPN mediates effects that lead to the accumulation of immune cells in the spleen and subsequent splenic enlargement.

C. rodentium Infection of Mouse Fibroblasts Results in Pedestal Formation

Intimate adherence of *C. rodentium* to wild-type mouse fibroblasts, but not cells from $OPN^{-/-}$ mice, was demon-

strated by transmission electron microscopy, with the formation of dense F-actin attachment pedestals after 4 hours of infection (Figure 5A), which is a pathognomonic feature of bacterial-induced A/E lesions.²² This is the first demonstration of *C. rodentium*-induced adherence pedestals, compatible with A/E lesions, in mouse-derived cells.²⁶

OPN Promotes *C. rodentium* and EHEC-Induced Pedestals

C. rodentium-infected wild-type mouse fibroblasts exhibited adhesion pedestals, as demonstrated by accumulation of dense F-actin-binding phalloidin at sites of bacterial attachment after 6 hours of infection. In contrast, pedestals were not observed in infected $OPN^{-/-}$ cells, indicating that OPN plays a role in bacterial-induced rearrangements of the host cell cytoskeleton. Furthermore, when human-OPN knock-in mouse fibroblasts were infected with *C. rodentium*, F-actin pedestals were observed (Figure 5B). Similar findings were also found after 4.5 hours infection of the 3 cell types with EHEC

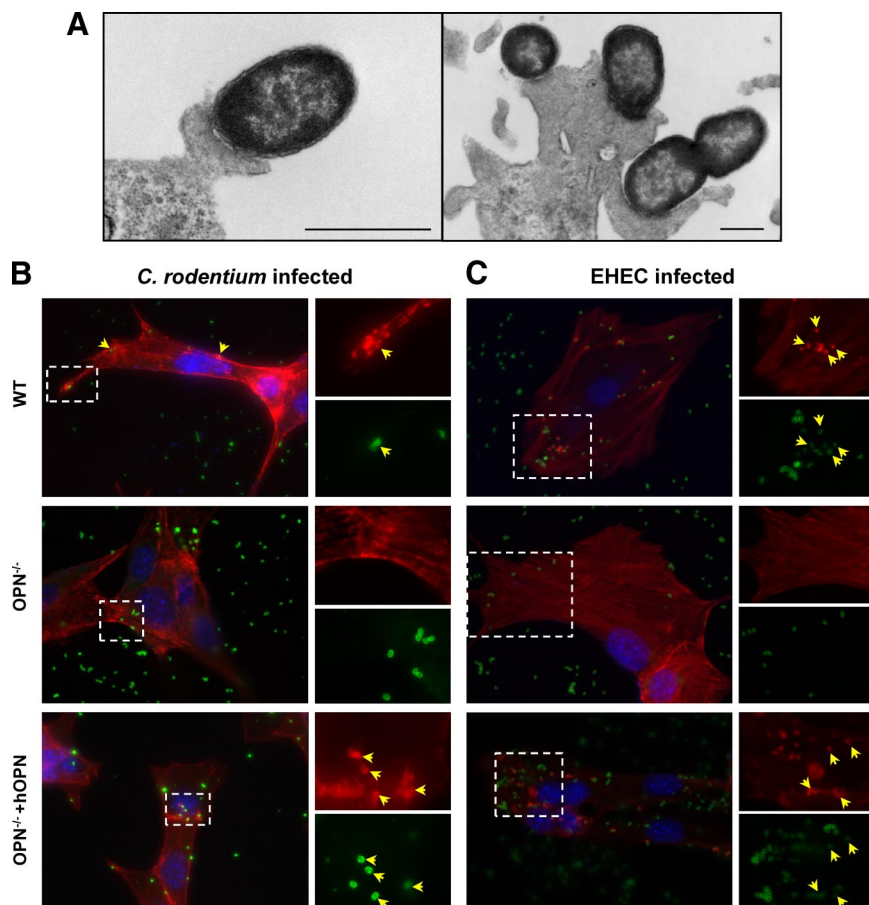


Figure 5. Formation of actin-dense attachment pedestals in mouse fibroblasts infected by *C. rodentium* and EHEC O157:H7 is mediated by OPN. **A:** Transmission electron photomicrographs of mouse fibroblasts infected for 4 hours at 37°C with *C. rodentium* demonstrate adhesion pedestals. Scale bar: 500 nm. **B:** *C. rodentium*-infected (bacteria stained green) wild-type (WT) mouse fibroblasts exhibited dense F-actin foci (stained with phalloidin, red), indicating formation of adhesion pedestals (arrowheads in top panels) and magnified insets corresponding with the outlined area). Pedestals were not present, however, in infected $OPN^{-/-}$ cells (middle panel and inset show adherent bacteria that are not accompanied by A/E lesions in the absence of OPN). Furthermore, when human OPN knock-in mouse fibroblasts were infected with *C. rodentium*, A/E-like lesions were again observed (bottom panel and insets). **C:** EHEC-infected cells were stained with fluorescein isothiocyanate-conjugated anti-EHEC (green), phalloidin (red), and DAPI (blue). Similar to *C. rodentium*, EHEC infection of wild-type fibroblasts induced adhesion pedestals (arrowheads in top panels), which were absent in infected $OPN^{-/-}$ cells (middle panels) and restored in human-OPN complemented $OPN^{-/-}$ fibroblasts (arrowheads in bottom panels).

(Figure 5C). This observation indicates that OPN is involved in formation of adhesion pedestals and that the role of OPN in response to *C. rodentium* infection can be extended to another intestinal pathogen containing the locus of enterocyte effacement pathogenicity island, EHEC O157:H7. There was also a 37% reduction in overall adhesion of *C. rodentium* to $OPN^{-/-}$ cells *in vitro* relative to wild-type fibroblasts ($P < 0.05$).

OPN status had no discernible effect on overall cell structure in uninfected fibroblasts. When $OPN^{-/-}$ cells were pretreated with either bovine milk-derived OPN or recombinant OPN, added to the medium, no pedestals were seen in response to EHEC infection (Figure 6). These findings suggest that an intracellular form of OPN mediates formation of pedestals, since addition of exogenous OPN to $OPN^{-/-}$ cells did not recover the

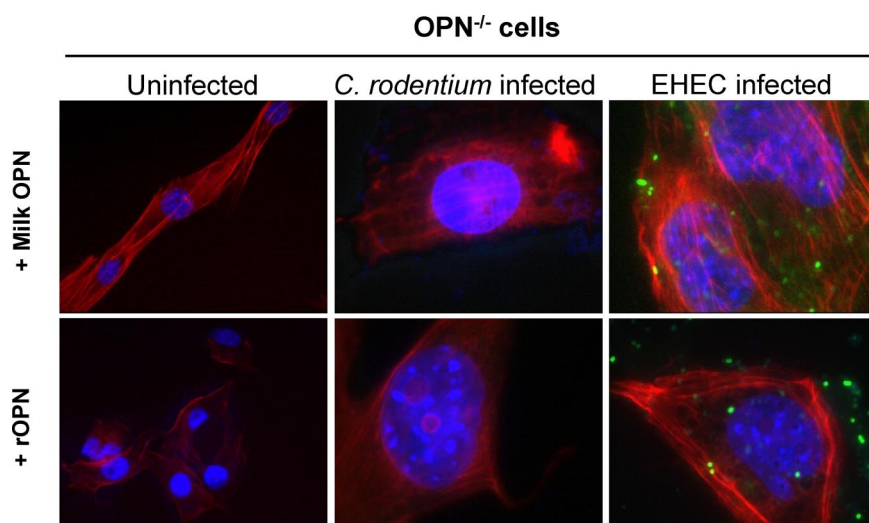


Figure 6. Exogenous OPN does not restore adhesion pedestals *in vitro*. Presence or absence of OPN had no effect on F-actin phalloidin staining (red) of uninfected fibroblasts (left column). Pretreatment of $OPN^{-/-}$ cells with extracellular, bovine milk-derived (top panels) or recombinant (bottom panels) OPN did not induce pedestals with infection, as demonstrated by multiple adherent bacteria (blue- *C. rodentium*; green- EHEC) without phalloidin-positive adhesion pedestals.

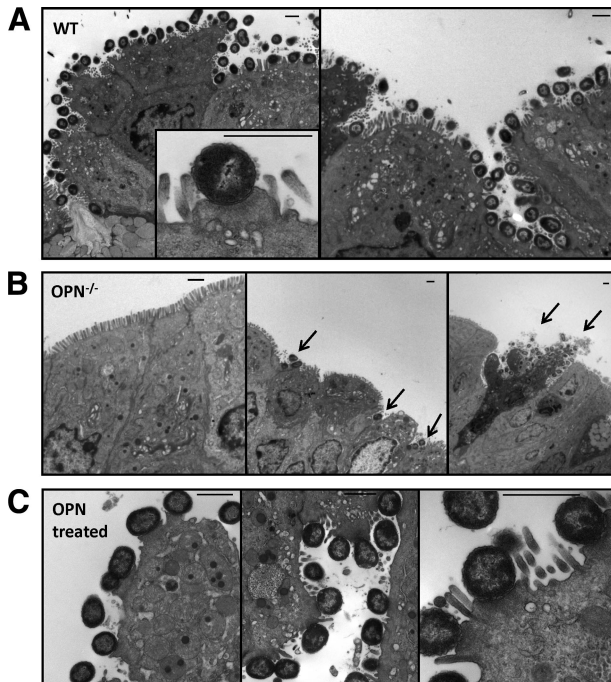


Figure 7. Actin-dense pedestals are formed in *C. rodentium*-infected wild-type (WT) mice and reduced in $OPN^{-/-}$ mice. **A:** Multiple bacteria carpeted the surface of colons of wild-type mice with A/E lesions after 6 days of infection with *C. rodentium*. **B:** In infected $OPN^{-/-}$ mice, there were no bacteria seen in most areas of the colon (left panel). In other areas, some adherent organisms were seen (arrows in middle panel), and only in rare cases were multiple adherent bacteria observed in infected $OPN^{-/-}$ mice, especially on shedding epithelial cells (arrows in right panel). **C:** $OPN^{-/-}$ mice treated with rectal OPN and infected with *C. rodentium* showed multiple A/E lesions.

wild-type phenotype *in vitro*. However, rectal OPN was able to recover the effect in $OPN^{-/-}$ mice.

To determine whether OPN is also involved in the formation of adhesion pedestals *in vivo*, colonic sections were examined 6 days after infection, at the time of maximum bacterial colonization (Figure 3C and ref. 24). While colons of wild-type mice were carpeted by multiple intimately adherent bacteria (Figure 7A), bacteria were absent from most colonic sections of $OPN^{-/-}$ mice and present only in small numbers in other areas (Figure 7B). Rarely, larger numbers of bacteria were found, located mainly in areas of mucosal damage and cell shedding (Figure 7B, right panel). Rectal administration of OPN restored A/E lesions, as shown by transmission electron microscopy (Figure 7C). Taken together, these results show that the formation of A/E lesions in response to bacterial infections is dependent on the presence of OPN.

Discussion

Due to recent controversies regarding the role of OPN in murine models of IBD,^{9–12} we evaluated the involvement of OPN in the development of intestinal changes in mice challenged with the murine enteric pathogen, *C. rodentium*. In the absence of OPN, mice were protected from bacterial colonization and the colonic epithelial hyperplastic cell response induced by *C. rodentium*. This protection correlated with a reduction in F-actin condensa-

tion directly below adherent *C. rodentium in vitro* and *in vivo*, indicating that the contribution of OPN to mucosal responses to infection could be, either directly or indirectly, mediated through bacterial attachment.

IBD, including Crohn's disease and ulcerative colitis, are chronic debilitating intestinal disorders characterized by mucosal inflammation.⁵ Increased levels of OPN are described in both the serum and intestinal mucosa of patients with IBD and correlate with disease severity.^{11,27} In these patients, OPN is produced by gut epithelia, IgG-producing plasma cells, and macrophages.^{28,29} Increased OPN expression in areas of active inflammation suggests that OPN is involved in stimulating cytokine production that contributes to a T_H1 -predominant adaptive immune response, as is observed in Crohn's disease.²¹ Since OPN is also associated with a decrease in the production of the anti-inflammatory cytokine IL-10 by T cells from patients with Crohn's disease,²⁸ OPN-mediated defects in immune-regulation may further contribute to the development of inflammation.

Most models studying the involvement of OPN in inflammation support a pro-inflammatory role for this key regulator, because disease is usually attenuated when OPN is absent. For example, OPN is elevated in the synovium of patients with rheumatoid arthritis and overexpression of OPN in synovial T cells amplifies inflammation.³⁰ $OPN^{-/-}$ mice with experimental autoimmune encephalomyelitis, as a T_H1 model of multiple sclerosis, are protected from disease,³¹ while administration of exogenous OPN causes relapse and paralysis.³² OPN is also involved in integrin adhesion,³³ inflammatory cell chemotaxis,³⁴ and in enhanced neutrophil function.³⁵ Our findings support a role for OPN in mediating immune responses to *C. rodentium* infection as demonstrated by a reduction in the increase of $IFN\gamma$ in $OPN^{-/-}$ mice.

Recent attempts to define a role for OPN in intestinal inflammation, using a chemically induced model of colitis (DSS), have yielded conflicting results. While our group has shown that $OPN^{-/-}$ mice are more susceptible to DSS colitis, through a reduction in tumor necrosis factor- α and neutrophil recruitment,^{10,12} other investigators found an opposite effect.⁹ More recently, Heilmann et al¹¹ found that $OPN^{-/-}$ mice are more susceptible to acute challenge with DSS, associated with reduced IL-22 and macrophage activity but increased serum tumor necrosis factor- α , while chronic DSS-induced colitis was reduced in these mice. This variability can be explained, at least in part, by the use of different mouse strains, OPN gene modification strategies, varying DSS doses, animal facility conditions, and treatment protocols. The reported discrepancies also highlight the limitations of the DSS model of colitis in mice and its applicability to IBD.³⁶ DSS exerts cytotoxic effects leading to breakdown of the mucosal barrier and exposure of the submucosal immune system to massive stimulation by luminal bacteria.³⁷ Resolution of inflammation in this model is mainly dependent on an ability to repair the breach, which is initiated by inflammation.³⁸ Since OPN is important in both neutrophil and fibroblast recruitment and in matrix deposition, which are essential for effective tissue repair,³⁹ it is not surprising that, in the absence of OPN, mice are more susceptible to

acute DSS colitis.^{10,11} Furthermore, as shown by increased mortality from chemical-induced colitis of rats treated with anti-L-selectin antibodies, neutrophil function has a protective effect in this setting.⁴⁰

Increases in spleen weight and splenocyte numbers seen in infected wild-type mice likely represent pooling of immune cells into the spleen in response to infection, as observed in mice infected with *Salmonella* Typhimurium.²⁵ Contrary to hindlimb-unloading, a chronic stress model where splenic atrophy is reduced in the absence of OPN,⁴¹ *C. rodentium* infection induced an increase in spleen mass and cellularity, which was prevented in OPN^{-/-} mice. The opposite effects of OPN on the spleen in these two settings can be explained by differences between the stress models. The former is a chronic immune suppression model, as indicated by increased serum corticosterone levels in wild-type, but not OPN^{-/-}-stressed mice,⁴¹ whereas the latter is a model of an acute, immune-mediated response to bacterial infection. In both cases, OPN serves as a central mediator of immune function that contributes to disease phenotype.

Our results clearly demonstrate that OPN^{-/-} mice are protected from the effects of *C. rodentium* infection, including colonic epithelial cell hyperplasia, histological changes, and bacterial translocation. In addition, the absence of OPN impaired the ability of *C. rodentium* to colonize the colons, which is likely why OPN^{-/-} mice are not as severely affected as wild-type-infected mice. However, while exogenous intrarectal OPN was able to restore some features in OPN^{-/-} mice, there was no detectable increase in colonization of these mice with *C. rodentium*. This discrepancy could be explained by only partial recovery of the wild-type phenotype with OPN administration to OPN^{-/-} mice (as shown for epithelial cell hyperplasia), a type II statistical error, or limitations of culture-based bacterial recovery methods used in this study. Since epithelial cell hyperplasia, pedestal formation, bacterial translocation to the liver, and splenic responses were all increased with rectal OPN treatment, the findings support a role for OPN in mediating responses to *C. rodentium* infection in this model.

OPN could either directly mediate bacterial attachment to host cells, as recently shown for Gram-positive bacteria,⁴² or modify host responses to bacteria. Alternatively, since adhesion and A/E lesion formation involve multiple complex host and microbial factors, it is possible that other mediators downstream to OPN could also explain these findings. For example, reduced inflammation in the absence of OPN could lead to a decrease in the abundance of epithelial attachment sites that are required for initial bacterial adhesion.⁴³ Since the highest increase in OPN was observed on PI day 10, it is more likely that OPN mediates signaling events related to A/E lesion formation and epithelial cell hyperplasia rather than being directly involved in bacterial attachment, which is observed earlier in the course of infection, around PI day 6.²²

Although *C. rodentium* is widely used to study enteric bacterial infections and intestinal inflammatory models,^{7,44} adhesion pedestals have not been demonstrated in mouse cells *in vitro*²⁶ or in human intestinal cells, unless *C. rodentium* is genetically modified to express a human

enteropathogen-derived bacterial adhesion.²⁶ To our knowledge, the intimately adherent bacteria *C. rodentium* and the accompanying F-actin-dense pedestals demonstrated in our study using immortalized mouse fibroblasts, are the first to show the formation of pedestals compatible with A/E lesions in response to *C. rodentium* infection in mouse cells. Furthermore, we found that the formation of bacterial-induced changes in the host cytoskeleton were absent in cells lacking OPN, and were restored by reintroducing human OPN into the cells, but not by pretreating cells with extracellular OPN. These findings indicate that OPN plays an important role in bacterial-induced attachment pedestal formation and suggest that an intracellular form of OPN mediates this effect since adding OPN to the medium was not sufficient to restore pedestals. In contrast, addition of topical OPN through rectal administration in OPN^{-/-} mice did restore effects of *C. rodentium* infection, possibly because OPN may be differentially processed and internalized in the *in vivo* setting. The ability of exogenous OPN to be absorbed and attenuate DSS-induced colitis¹² supports a potential use for this compound in future research.

C. rodentium attachment to cells involves either locus of enterocyte effacement-dependent (involved in A/E lesion formation) or locus of enterocyte effacement-independent mechanisms. Since OPN was involved in pedestal formation, this likely provides the mechanism for reduced pathogen colonization and less severe colonic involvement in OPN^{-/-} mice. A specific reduction in the formation of adhesion pedestals and in overall adhesion *in vitro* supports a role for actin rearrangements in anchoring bacteria and stabilizing colonization, as demonstrated by the failure of *espF_u*^{-/-} EHEC to persist colonization in rabbits due to reduction in A/E lesions.⁴⁵ Furthermore, the OPN receptor CD44 is recruited to pedestals on EHEC infection, although, in contrast to OPN, A/E lesions are still formed in the absence of this host protein.⁴⁶ These findings suggest that CD44 is not functional in the formation of pedestals, whereas our results indicate that OPN is. Further *in vivo* evidence supporting a role for OPN in the formation of adherence pedestals is provided by a reduction in A/E lesions in OPN^{-/-} mice on PI day 6, which is likely the cause of the reduced colonization. Alternatively, it is also possible that OPN has a more profound effect on the composition of the intestinal microbiota, although this was not directly addressed in this paper. This possibility is supported by the recent description of reduced *C. rodentium* colonization and reduced epithelial cell hyperplasia when mice are colonized with a single commensal microbe.⁴⁷

Defects in migration of cells in the absence of OPN, such as shown for neutrophil recruitment³⁵ and macrophage chemotaxis,³⁴ are mediated by impaired cytoskeletal responses, likely due to a reduction in association with the CD44 receptor.^{39,48} Furthermore, while unchallenged OPN-null fibroblasts exhibit a normal cytoskeleton, stressed cells show defects in rearrangements of the actin cytoskeleton and in the ability to form stress fibers and focal adhesions.⁴⁹ Similarly, our findings suggest a role for OPN in modulating host responses to intestinal bacteria in infected epithelial cells, which then specifi-

cally impacts on the development of mucosal injury and responses to enteric pathogens.

Taken together, these findings indicate that OPN is required and sufficient for the formation of pedestals in response to bacterial infection, explaining why OPN^{-/-} mice are protected from the colonic changes typically seen in response to this non-invasive, enteric bacterial infection. This provides a rationale for future studies on the role of OPN in mediating bacterial attachment to gut epithelia in humans with IBD.

Acknowledgments

We thank Lei Liu (University of Alberta) for technical assistance; Michael Ho and Yew Meng Heng (Department of Pediatric Laboratory Medicine, Hospital for Sick Children) for their expertise in microscopy techniques; and Kelvin So (Toronto General Hospital) for immunostaining. OPN^{-/-} mice were originally provided by Dr. Susan R. Rittling, (Forsyth Institute, Boston, MA) and Dr. David T. Denhardt (Rutgers University, Piscataway, NJ).

References

1. Hashimoto M, Sun D, Rittling SR, Denhardt DT, Young W: Osteopontin-deficient mice exhibit less inflammation, greater tissue damage, and impaired locomotor recovery from spinal cord injury compared with wild-type controls. *J Neurosci* 2007, 27:3603–3611
2. Scatena M, Liaw L, Giachelli CM: Osteopontin: a multifunctional molecule regulating chronic inflammation and vascular disease. *Arterioscler Thromb Vasc Biol* 2007, 27:2302–2309
3. Morimoto J, Inobe M, Kimura C, Kon S, Diao H, Aoki M, Miyazaki T, Denhardt DT, Rittling S, Uede T: Osteopontin affects the persistence of beta-glucan-induced hepatic granuloma formation and tissue injury through two distinct mechanisms. *Int Immunol* 2004, 16:477–488
4. Neish AS: Microbes in gastrointestinal health and disease. *Gastroenterology* 2009, 136:65–80
5. Xavier RJ, Podolsky DK: Unravelling the pathogenesis of inflammatory bowel disease. *Nature* 2007, 448:427–434
6. Deng W, Vallance BA, Li Y, Puente JL, Finlay BB: Citrobacter rodentium translocated intimin receptor (Tir) is an essential virulence factor needed for actin condensation, intestinal colonization and colonic hyperplasia in mice. *Mol Microbiol* 2003, 48:95–115
7. Eckmann L: Animal models of inflammatory bowel disease: lessons from enteric infections. *Ann NY Acad Sci* 2006, 1072:28–38
8. Borenshtein D, McBee ME, Schauer DB: Utility of the Citrobacter rodentium infection model in laboratory mice. *Curr Opin Gastroenterol* 2008, 24:32–37
9. Zhong J, Eckhardt ER, Oz HS, Bruemmer D, de Villiers WJ: Osteopontin deficiency protects mice from Dextran sodium sulfate-induced colitis. *Inflamm Bowel Dis* 2006, 12:790–796
10. da Silva AP, Pollett A, Rittling SR, Denhardt DT, Sodek J, Zohar R: Exacerbated tissue destruction in DSS-induced acute colitis of OPN-null mice is associated with downregulation of TNF-alpha expression and non-programmed cell death. *J Cell Physiol* 2006, 208:629–639
11. Heimann K, Hoffmann U, Witte E, Loddenkemper C, Sina C, Schreiber S, Hayford C, Holzlohner P, Wolk K, Tchatchou E, Moos V, Zeitl M, Sabat R, Gunther U, Wittig BM: Osteopontin as two-sided mediator of intestinal inflammation. *J Cell Mol Med* 2008, 13:1162–1174
12. da Silva AP, Ellen RP, Sorensen ES, Goldberg HA, Zohar R, Sodek J: Osteopontin attenuation of dextran sulfate sodium-induced colitis in mice. *Lab Invest* 2009, 89:1169–1181
13. Rittling SR, Matsumoto HN, McKee MD, Nanci A, An XR, Novick KE, Kowalski AJ, Noda M, Denhardt DT: Mice lacking osteopontin show normal development and bone structure but display altered osteoclast formation in vitro. *J Bone Miner Res* 1998, 13:1101–1111
14. Schack L, Lange A, Kelsen J, Agnholt J, Christensen B, Petersen TE, Sorensen ES: Considerable variation in the concentration of osteopontin in human milk, bovine milk, and infant formulas. *J Dairy Sci* 2009, 92:5378–5385
15. Van der Sluis M, De Koning BA, De Bruijn AC, Velcich A, Meijerink JP, Van Goudoever JB, Buller HA, Dekker J, Van Seuningen I, Renes IB, Einerhand AW: Muc2-deficient mice spontaneously develop colitis, indicating that MUC2 is critical for colonic protection. *Gastroenterology* 2006, 131:117–129
16. LeBlanc PM, Yeretssian G, Rutherford N, Doiron K, Nadiri A, Zhu L, Green DR, Gruenheid S, Saleh M: Caspase-12 modulates NOD signaling and regulates antimicrobial peptide production and mucosal immunity. *Cell Host Microbe* 2008, 3:146–157
17. Zohar R, Zhu B, Liu P, Sodek J, McCulloch CA: Increased cell death in osteopontin-deficient cardiac fibroblasts occurs by a caspase-3-independent pathway. *Am J Physiol Heart Circ Physiol* 2004, 287:H1730–H1739
18. Sorensen ES, Petersen TE: Purification and characterization of three proteins isolated from the proteose peptone fraction of bovine milk. *J Dairy Res* 1993, 60:189–197
19. Hunter GK, Grohe B, Jeffrey S, O'Young J, Sorensen ES, Goldberg HA: Role of phosphate groups in inhibition of calcium oxalate crystal growth by osteopontin. *Cells Tissues Organs* 2009, 189:44–50
20. Qu-Hong, Dvorak AM: Ultrastructural localization of osteopontin immunoreactivity in phagolysosomes and secretory granules of cells in human intestine. *Histochem J* 1997, 29:801–812
21. Sato T, Nakai T, Tamura N, Okamoto S, Matsuoka K, Sakuraba A, Fukushima T, Uede T, Hibi T: Osteopontin/Eta-1 upregulated in Crohn's disease regulates the Th1 immune response. *Gut* 2005, 54:1254–1262
22. Mundy R, MacDonald TT, Dougan G, Frankel G, Wiles S: Citrobacter rodentium of mice and man. *Cell Microbiol* 2005, 7:1697–1706
23. Vallance BA, Deng W, Jacobson K, Finlay BB: Host susceptibility to the attaching and effacing bacterial pathogen Citrobacter rodentium. *Infect Immun* 2003, 71:3443–3453
24. Borenshtein D, Nambiar PR, Groff EB, Fox JG, Schauer DB: Development of fatal colitis in FVB mice infected with Citrobacter rodentium. *Infect Immun* 2007, 75:3271–3281
25. Berntman E, Rolf J, Johansson C, Anderson P, Cardell SL: The role of CD1d-restricted NK T lymphocytes in the immune response to oral infection with Salmonella typhimurium. *Eur J Immunol* 2005, 35:2100–2109
26. Tobe T, Sasakawa C: Species-specific cell adhesion of enteropathogenic Escherichia coli is mediated by type IV bundle-forming pili. *Cell Microbiol* 2002, 4:29–42
27. Masuda H, Takahashi Y, Asai S, Takayama T: Distinct gene expression of osteopontin in patients with ulcerative colitis. *J Surg Res* 2003, 111:85–90
28. Agnholt J, Kelsen J, Schack L, Hvas CL, Dahlerup JF, Sorensen ES: Osteopontin, a protein with cytokine-like properties, is associated with inflammation in Crohn's disease. *Scand J Immunol* 2007, 65:453–460
29. Gordon JN, MacDonald TT: Osteopontin: a new addition to the constellation of cytokines which drive T helper cell type 1 responses in Crohn's disease. *Gut* 2005, 54:1213–1215
30. Xu G, Nie H, Li N, Zheng W, Zhang D, Feng G, Ni L, Xu R, Hong J, Zhang JZ: Role of osteopontin in amplification and perpetuation of rheumatoid synovitis. *J Clin Invest* 2005, 115:1060–1067
31. Chabas D, Baranzini SE, Mitchell D, Bernard CC, Rittling SR, Denhardt DT, Sobel RA, Lock C, Karpuz M, Pedotti R, Heller R, Oksenberg JR, Steinman L: The influence of the proinflammatory cytokine, osteopontin, on autoimmune demyelinating disease. *Science* 2001, 294:1731–1735
32. Hur EM, Youssef S, Haws ME, Zhang SY, Sobel RA, Steinman L: Osteopontin-induced relapse and progression of autoimmune brain disease through enhanced survival of activated T cells. *Nat Immunol* 2007, 8:74–83
33. Kon S, Ikesue M, Kimura C, Aoki M, Nakayama Y, Saito Y, Kurotaki D, Diao H, Matsui Y, Segawa T, Maeda M, Kojima T, Uede T: Syndecan-4 protects against osteopontin-mediated acute hepatic injury by masking functional domains of osteopontin. *J Exp Med* 2008, 205:25–33
34. Zhu B, Suzuki K, Goldberg HA, Rittling SR, Denhardt DT, McCulloch CA, Sodek J: Osteopontin modulates CD44-dependent chemotaxis of peritoneal macrophages through G-protein-coupled receptors: evi-

- dence of a role for an intracellular form of osteopontin. *J Cell Physiol* 2004, 198:155–167
35. Koh A, da Silva AP, Bansal AK, Bansal M, Sun C, Lee H, Glogauer M, Sodek J, Zohar R: Role of osteopontin in neutrophil function. *Immunology* 2007, 122:466–475
36. Kawada M, Arihiro A, Mizoguchi E: Insights from advances in research of chemically induced experimental models of human inflammatory bowel disease. *World J Gastroenterol* 2007, 13:5581–5593
37. Wirtz S, Neufert C, Weigmann B, Neurath MF: Chemically induced mouse models of intestinal inflammation. *Nat Protoc* 2007, 2:541–546
38. Khalil PN, Weiler V, Nelson PJ, Khalil MN, Moosmann S, Mutschler WE, Siebeck M, Huss R: Nonmyeloablative stem cell therapy enhances microcirculation and tissue regeneration in murine inflammatory bowel disease. *Gastroenterology* 2007, 132:944–954
39. Sodek J, Batista Da Silva AP, Zohar R: Osteopontin and mucosal protection. *J Dent Res* 2006, 85:404–415
40. Kuhl AA, Kakirman H, Janotta M, Dreher S, Cremer P, Pawlowski NN, Loddenkemper C, Heimesaat MM, Grollich K, Zeitz M, Farkas S, Hoffmann JC: Aggravation of different types of experimental colitis by depletion or adhesion blockade of neutrophils. *Gastroenterology* 2007, 133:1882–1892
41. Wang KX, Shi Y, Denhardt DT: Osteopontin regulates hindlimb-unloading-induced lymphoid organ atrophy and weight loss by modulating corticosteroid production. *Proc Natl Acad Sci* 2007, 104:14777–14782
42. Schack L, Stapulionis R, Christensen B, Kofod-Olsen E, Skov Sorensen UB, Vorup-Jensen T, Sorensen ES, Hollsberg P: Osteopontin enhances phagocytosis through a novel osteopontin receptor, the alphaXbeta2 integrin. *J Immunol* 2009, 182:6943–6950
43. Higgins LM, Frankel G, Connerton I, Goncalves NS, Dougan G, MacDonald TT: Role of bacterial intimin in colonic hyperplasia and inflammation. *Science* 1999, 285:588–591
44. Frankel G, Phillips AD: Attaching effacing *Escherichia coli* and paradigms of Tir-triggered actin polymerization: getting off the pedestal. *Cell Microbiol* 2008, 10:549–556
45. Ritchie JM, Brady MJ, Riley KN, Ho TD, Campellone KG, Herman IM, Donohue-Rolfe A, Tzipori S, Waldor MK, Leong JM: EspFU, a type III-translocated effector of actin assembly, fosters epithelial association and late-stage intestinal colonization by *E. coli* O157:H7. *Cell Microbiol* 2008, 10:836–847
46. Goosney DL, DeVinney R, Finlay BB: Recruitment of cytoskeletal and signaling proteins to enteropathogenic and enterohemorrhagic *Escherichia coli* pedestals. *Infect Immun* 2001, 69:3315–3322
47. Ivanov II, Atarashi K, Manel N, Brodie EL, Shima T, Karaoz U, Wei D, Goldfarb KC, Santee CA, Lynch SV, Tanoue T, Imaoka A, Itoh K, Takeda K, Umesaki Y, Honda K, Littman DR: Induction of intestinal Th17 cells by segmented filamentous bacteria. *Cell* 2009, 139:485–498
48. Collins CB, Ho J, Wilson TE, Wermers JD, Tlaxca JL, Lawrence MB, Solga M, Lannigan J, Rivera-Nieves J: CD44 deficiency attenuates chronic murine ileitis. *Gastroenterology* 2008, 135:1993–2002
49. Lenga Y, Koh A, Perera AS, McCulloch CA, Sodek J, Zohar R: Osteopontin expression is required for myofibroblast differentiation. *Circ Res* 2008, 102:319–327